World Applied Sciences Journal 11 (1): 06-11, 2010
ISSN 1818-4952
© IDOSI Publications, 2010

Analysis of Dynamic Characteristics of Self-Assembled Quantum Dot Lasers

[1]A.S. Naeimi, [2]Davoud Ghodsi Nahri and [1]S.A. Kazemipour

[1]Islamic Azad University, Aliabad Katoul Branch, Iran
[2]Department of Physics, Faculty of Science,
Islamic Azad University, Mashhad Branch, Mashhad, Iran

Abstract: We have solved the rate equations of self-assembled quantum-dot lasers considering homogeneous and inhomogeneous broadenings of linear optical gain numerically using fourth-order Runge-Kutta method. Dynamic-characteristics of InGaAs/GaAs self-assembled quantum-dot lasers are analyzed; we show that turn-on delay and relaxation oscillation frequency improve as injected current increases. Enhancing the homogeneous broadening results in increasing threshold current and turn-on delay and decreasing relaxation oscillation frequency. We also show that uncompleted steady-states appear at photon-time characteristics at homogeneous broadenings comparable or equal to inhomogeneous broadening. There is a special homogeneous broadening for a given injected current which the QD laser has its best output power. It is also shown that for larger phonon bottlenecks and inhomogeneous broadenings, turn-on delay increases and uncompleted steady-state photons decline.

Key words: Quantum-dot laser • Inhomogeneous and homogeneous broadenings • Dynamic-characteristics

INTRODUCTION

The emergence of devices based on nanometer-size active elements marked the era of nanoelectronics and nanophotonics. Among such elements are notably low-dimensional heterostructures, such as quantum wells (QWs), quantum wires (QWRs) and quantum dots (QDs). Quantum confinement in low-dimensional heterostructure strongly modifies the basic properties of a semiconductor crystal.

In QDs carriers are three-dimensionally confined and the modification of electronic properties is quite stronger than QWs and QWRs. In QDs, the energy levels are discrete and transitions between electrons and holes are comparable with transitions between discrete levels of single atoms. Thus, QDs are also referred to as superatoms or artificial atoms [1].

Semiconductor laser is the fundamental device of modern optoelectronics and photonics. Due to unique three dimensional quantum confinement, QD lasers have demonstrated both theoretically and experimentally many superior properties, such as ultra-low and temperature-stable threshold current density, high optical gain, high-speed operation, broad modulation bandwidth and narrow spectrum linewidth primarily due to the delta-functionlike density of states [2, 3]. However, we know that actual self-assembled QDs do not always meet our expectation because of the inhomogeneous and homogeneous broadenings of the optical gain and phonon bottleneck. Thus, for an accurate and rigorous analysis of QD-LDs we need to take into account all these actual aspects of QDs [4].

In this paper, first, we describe analyzing theory of QD laser based on the rate equation model and consider the homogeneous and inhomogeneous broadenings of the linear optical gain for solving InGaAs/GaAs self-assembled quantum dot laser (SAQD-LD) rate equations numerically using fourth-order Runge-Kutta method. Then, in the result section, we achieve dynamic response and analyze carrier and photon-time characteristics of the mentioned QD laser at different injected currents and different homogeneous broadenings, In addition, the effects of initial relaxation lifetime (phonon bottleneck) and inhomogeneous broadening on dynamic characteristics are treated.

Optical Gain Theory: Based on the density-matrix theory, the linear optical gain of QD active region is given as [5].

Corresponding Author: A.S.Naeimi, Islamic Azad University, Aliabad Katoul Branch, Iran.

$$g^{(1)}(E) = \frac{2\pi e^2 \hbar N_D}{c n_r \varepsilon_0 {m_0}^2} \sum_{c,v} \frac{|P_{cv}^{\sigma}|^2 (f_c - f_v)}{E_{cv}} B_{cv}(E - E_{cv}) \quad (1)$$

Where n_r is the refractive index, N_D is the volume density of QDs, $|P_{cv}^{\sigma}|^2$ is the transition matrix element, f_c is the electron occupation function of the conduction-band discrete state, f_v is that of the valence-band discrete state and E_{cv} is the interband transition energy. The linear optical gain shows the homogeneous broadening of a Lorentz shape as.

$$B_{cv}(E - E_{cv}) = \frac{h\Gamma_{cv}/\pi}{(E - E_{cv})^2 + (h\Gamma_{cv})^2} \quad (2)$$

Where FWHM is given as $2\hbar\Gamma_{cv}$ with polarization dephasing or scattering rate Γ_{cv}. Neglecting the optical-field polarization dependence, the transition matrix element is given as

$$|P_{cv}^{\sigma}|^2 = |I_{cv}|^2 M^2 \quad (3)$$

Where I_{cv} represents the overlap integral between the envelope functions of an electron and a hole and

$$M^2 = \frac{{m_0}^2}{12{m_e}^*} \frac{E_g(E_g + \Delta)}{E_g + 2\Delta/3} \quad (4)$$

as derived by the first-order k.p interaction between the conduction band and valence band. Here, E_g is the band gap, m_e* is the electron effective mass, Δ is the spin-orbit interaction energy of the QD material. Equation (3) holds as long as we consider QDs with a nearly symmetrical shape.

In actual SAQD-LDs, we should rewrite the linear optical gain formula of Eq. (1) by taking into account inhomogeneous broadening due to the QD size and composition fluctuation in terms of a convolution integral as

$$g^{(1)}(E) = \frac{2\pi e^2 \hbar N_D}{c n_r e_0 {m_0}^2} \sum_{c,v} \frac{|P_{cv}^{s}|^2}{E_{cv}} \int_{-\infty}^{\infty} \left(f_c(E') - f_v(E')\right) \times B_{cv}(E - E') G(E' - E_{cv}) dE' \quad (5)$$

Where E_{cv} is the center of the energy distribution function of each interband transition, $f_c(E')$ is the electron occupation function of the conduction-band discrete state of the QDs with the interband transition energy of E' and $f_c(E')$ is that of the valence band discrete state. The energy fluctuation of QDs are represented by $G(E' - E_{cv})$ that takes a Gaussian distribution function as

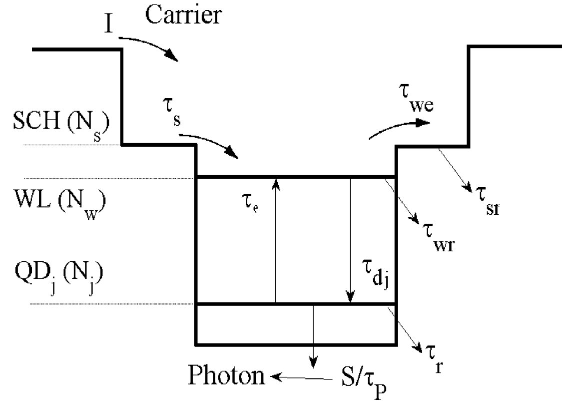

Fig. 1: Energy diagram of the laser-active region and diffusion, recombination and relaxation processes

$$G(E' - E_{cv}) = \frac{1}{\sqrt{2\pi}\xi_0} \exp\left[-(E' - E_{cv})^2 / 2{\xi_0}^2\right] \quad (6)$$

Whose FWHM is given by $\Gamma_0 = 2.35\xi_0$ The width Γ_0 usually depends on the band index *c* and *v* [6].

Rate Equations: The most popular and useful way to deal with carrier and photon dynamics in lasers is to solve rate equations for carrier and photons. Fig. 1 illustrates the energy diagram of the conduction band of the self-assembled quantum dot laser active region and diffusion, relaxation, recombination and escape processes of carriers [6, 7]. We consider an electron and a hole as an exciton, thus, the relaxation means the process that both an electron and a hole relax into the ground state simultaneously to form an exciton. We assume that only a single discrete electron and hole ground state is formed inside the QD and the charge neutrality always holds in each QD, i.e., $f_c(E') = 1 - f_v(E')$.

In order to describe the interaction between the QDs with different resonant energies through photons, we divide the QD ensemble into *j=1, 2,... 2M+1* groups, depending on their resonant energy for the interband transition, over the longitudinal cavity photon modes. *j* = *M* corresponds to the group and mode at E_{cv}. We take the energy width of each group equal to the mode separation of the longitudinal cavity photon modes which equals to

$$\Delta E = ch/(2n_r L_{ca}) \quad (7)$$

Where L_{ca} is the cavity length. The energy of the *j*th QDs group is represented by

$$Ej = Ecv - (M - j)\Delta E \quad (8)$$

Where $j = 1,2,...,2M+1$. The QD density jth QDs group is given as

$$N_D G_j = N_D G(E_j - E_{cv})\Delta E \quad (9)$$

Where ND is QD volume density. Let N_j be the carrier number in jth QDs group, According to Pauli's exclusion principle, the occupation probability in the ground state of the jth QDs group is defined as

$$P_j = N_j/(2N_D V_a G_j) \quad (10)$$

Where V_a is the total active region volume.
The rate equations are as follows [4-9]

$$dN_s//dt = I/e - N_s/\tau_s - N_s/\tau_{rs} + N_w/\tau_{we} \quad (11)$$

$$dN_w/dt = N_s/t_s + \sum_j N_j/t_e D_g - N_w/t_{wr} - N_w/t_{we} - N_w/\overline{t}_d \quad (12)$$

$$dN_j/dt = N_w G_j/t_{dj} - N_j/t_r - N_j/t_e D_g - \frac{cG}{n_r}\sum_m g^{(1)} S_m \quad (13)$$

$$dS_m/dt = \beta N_j/t_r + \frac{cG}{n_r}\sum_j g^{(1)} S_m - S_m/t_p \quad (14)$$

Where N_s, N_w and N_j are the carrier number in SCH layer, wetting layer (WL) and jth QDs group, respectively, S_m is the photon number of mth mode, where $m=1,2...2M+1$, I is the injected current, G_j is the fraction of the jth QDs group type within an ensemble of different dot size populations, e is the electron charge, D_g is the degeneracy of the QD ground state without spin, β is the spontaneous-emission coupling efficiency to the lasing mode. g_{mj} is the linear optical gain which the jth QDs group gives to the mth mode photons where is represented by

$$g_{mj}^{(1)} = \frac{2pe^2 hN_D}{cn_r e_0 m_0^2}\frac{|P_{cv}^s|^2}{E_{cv}}(2P_j - 1)G_j B_{cv}(E_m - E_j) \quad (15)$$

The related time constants are, τ_s diffusion in the SCH region, τ_{sr} carrier recombination in the SCH region, τ_{we}, carrier reexcitation from the WL to the SCH region, τ_{wr}, carrier recombination in the WL, τ_{dj}, carrier relaxation into the jth QDs group, τ_r, carrier recombination in the QDs, τ_p, photon lifetime in the cavity, The average carrier relaxation lifetime, $\overline{\tau}_d$, is given as

Table 1: Parameters Used for Simulation of Ingas/gaas Saqd-ld [6]

Parameter		Value
R	Radius of QD	$8nm$
h	Height of QD	$8nm$
E_{cv}	Interband transition energy	$1eV$
VD	Volume of QD	$\pi R^2 h$
ξ	Coverage of QDs	20%
NW	Number of QD layer	3
Γ	Optical confinement factor	4%
R_1,R_2	Mirror reflectivities	30%, 90%
α	Internal loss	$6cm^{-6}$
d	Stripe width	$10\mu m$
V_a	is the total active region volume	2.16×10^{-16}
τ_p	Photon cavity lifetime	$8.8ps$
L_{cav}	Cavity length	$900\mu m$
Γ_0	FWHM of inhomogeneous broadening	$20meV$
τ_0	Initial carrier relaxation lifetime	$10ps$
Δ	Spin-orbit interaction energy	$0.35eV$
m_e^*	Electron effective mass	$0.04m_0$
β	Spontaneous-emission coupling efficiency	10^{-4}
n_r	Refractive index	3.5
E_g	Band gap of bulk semiconductor	$0.8eV$
τ_s	Diffusion lifetime in the SCH region	$15ps$
τ_{wr}	Carrier recombination lifetime in the WL	$3ns$
τ_r	Carrier recombination lifetime in the QDs	$2.8ns$

$$\overline{t}_d^{-1} = \sum_n t_{dn}^{-1} G_n = \sum_n t_o^{-1}(1 - P_n)G_n \quad (16)$$

Where τ_0 is the initial carrier relaxation lifetime. The photon lifetime in the cavity is

$$t_p^{-1} = (c/n_r)\left[\alpha_i + \ln(1/R_1 R_2)/(2L_{cav})\right] \quad (17)$$

Where R_1 and R_2 are the cavity mirror reflectivities and α_i is the internal loss. The laser output power of the mth mode from one cavity mirror is given as

$$I_m = \hbar\omega_m c S_m \ln(1/R)/(2L_{cav} n_r) \quad (18)$$

Where ω_m is the emitted photon frequency and R is R_1 or R_2.

We solved the rate equations numerically using fourth-order Runge-Kutta method to obtain the carrier and photon characteristics. We assume that all the carriers are injected into the WL, i.e., $\tau_{sr} = \tau_{we}$ and consider the thermal carrier escape time $\tau_e = \infty$. It is assumed that QDs have a cylindrical shape. The parameters that we used at simulation are listed in Table 1 [6].

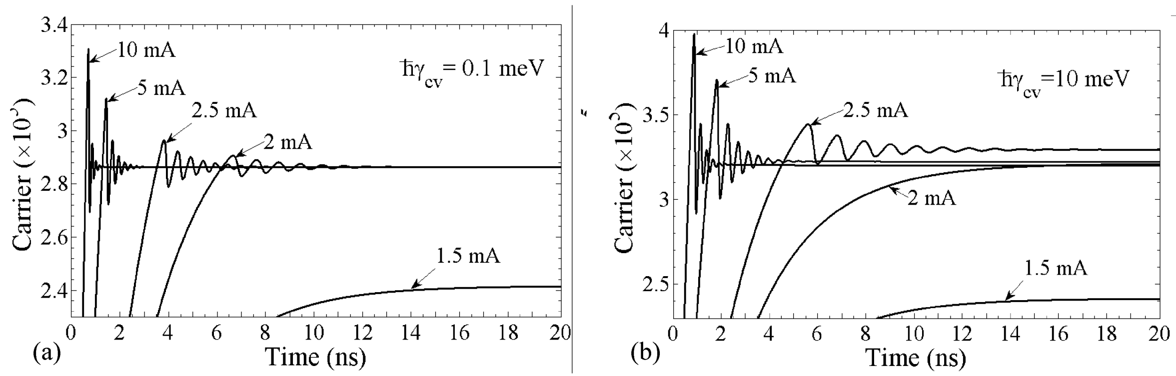

Fig. 2: Simulated results of carrier-time characteristics for different injection currents I=1.5, 2, 2.5, 5, and 10 mA at the FWHM of homogeneous broadenings (a) $\hbar\gamma_{cv}$ = 0.1 *meV* and (b) 10 *meV*

Fig. 3: Simulated results of photon-time characteristics for different injected currents I=2, 2.5, 5, and 10 mA when (a) $\hbar\gamma_{cv}$ = 0.1*meV*, (b) 1*meV*, (c)3*meV*, (d) 5*meV*, (e) 7*meV* and (f) 10*meV*

Simulation Results: We have solved the rate equations (11) to (14) using numeric method of Runge-Kutta. Fig. 2 shows the simulation results of carrier-characteristics for different injection currents I=1.5, 2, 2.5, 5 and 10 mA at the FWHM of homogeneous broadenings (a) $2\hbar\gamma_{cv} = 0.2meV$ and (b) $\hbar\gamma_{cv} = 20meV$.

As shown in Fig. 2, increasing the injection current, turn on delay decreases, relaxation oscillation peak and relaxation oscillation frequency enhance. In addition, relaxation oscillation peak, except for I=2 mA, increases and relaxation oscillation frequency degrades for larger homogeneous broadenings.

Fig. 3 shows the simulated results of photon-time characteristics for different injection currents I=2, 2.5, 5 and 10 mA when the FWHM of homogeneous broadening is (a) $2\hbar\gamma_{cv} = 0.2meV$, (b) $2meV$ (c) $6meV$ (d) $10meV$, (e) $14meV$ and (f) $20meV$.

As shown in Fig. 3, in some cases like Fig. 3(d), 3(e) and 3(f) that homogeneous broadening is comparable or equal to Inhomogeneous broadening at I =5 and 10 mA, photon numbers do not completely reach the steady-state after finishing the relaxation oscillation and continue to increase or decrease as the time increases. Consequently, we use uncompleted steady-state to point these states. The uncompleted steady-state photons, except for Fig. 3(d), elevate as the injected current increases. This is because, with increase of the injected current, at first, the QDs' carriers increase that results in enhancement of the cavity lasing photons, these increased photons that we call early photons lead to elevating the stimulated emission rate, consequently, the QDs' carriers decrease (Fig. 2) and the lasing photons heighten.

Increasing of the injected current, turn on delay decreases, this occurs because, required carriers for starting the relaxation oscillation are supplied sooner. Relaxation oscillation frequency and relaxation oscillation peak also enhance because additional increase of early photons leads to further enhancement of relaxation oscillation peak. On the other hand, increasing of the stimulated emission rate leads to the sooner light-amplification and decreasing of the cavity photons' lifetime, therefore, the relaxation oscillation frequency increases and the laser reaches the uncompleted steady-state quicker.

As the homogeneous broadening heightens from (a) to (f),

turn on delay enhances, because DOS of the central group elevates and energy levels are broadened, therefore the number of carriers required for beginning of lasing increases and are supplied later. (Uncompleted) steady-state photons at I=5 and 10 mA, except to Fig. 3(d), increase due to the enhancement of the QD groups within the homogeneous broadening of the central mode and as a result, increasing the carriers emitting within the central mode, while emitting of the central group carriers within the other modes at the currents I=5 and 10 mA (Fig. 3(d)) results in decreasing of the central mode (uncompleted) steady-state photons. Furthermore, threshold current increases because lasing emission decline as it completely vanishes at homogeneous broadening 20 meV.

Fig. 4 Shows the photon-time characteristics for I=2 mA at (a) $2\hbar\gamma_{cv} = 0.1,1, 3, 5\ and\ 7meV$ (b) $\hbar\gamma_{cv} = 7, 7.5, 8.5\ and\ 10meV$.

Enhancing of the homogeneous broadening toward a special value for a specific current (for example, in Fig. 4(a), 6 meV ($\hbar\gamma_{cv} = 3meV$)) leads to increasing of the relaxation oscillation peak and uncompleted steady-state photon numbers because of enhancement of central group DOS of Qds and as a result, the carriers emitting within the central mode. Further enhancement of

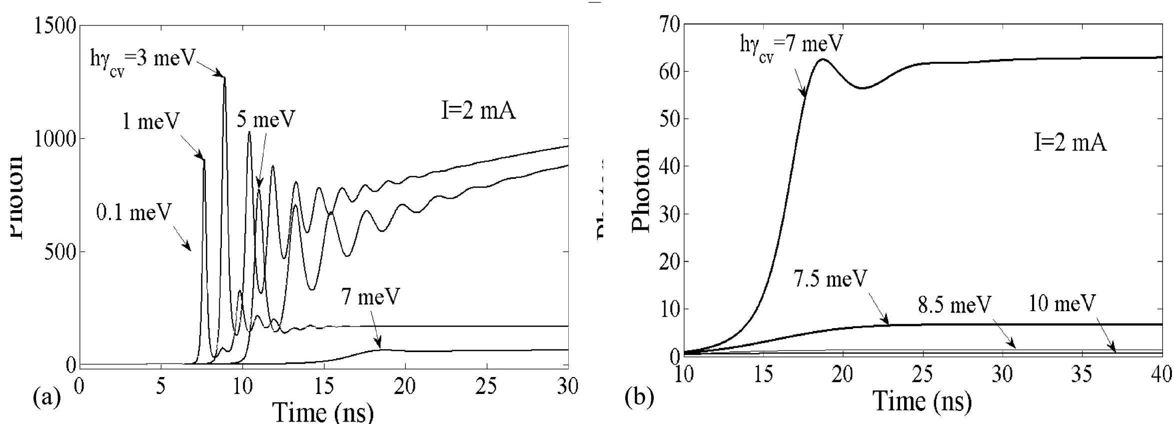

Fig. 4: Photon-time characteristics for I=2 mA at (a) $\hbar\gamma_{cv} = 0.1,1, 3, 5,\ and\ 7meV$ and (b) $\hbar\gamma_{cv} = 7, 7.5, 8.5\ and\ 10meV$,

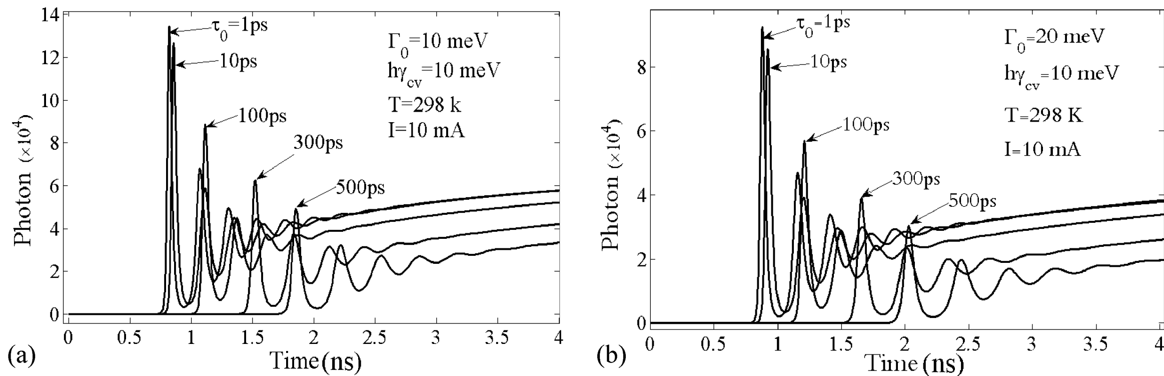

Fig. 5: The output photon dynamics at RT with carrier relaxation lifetime as a parameter for different inhomogeneous broadening- FWHMs (a) 10 meV and (b) 20 meV.

the homogeneous broadening, on the other hand, results in increasing the empty DOS at the central group and, accordingly, an inverse phenomenon that is, decreasing the population inversion. In fact, there is a best homogeneous broadening for a special injected current that the laser reveals the best performance.

Fig. 5 shows the room-temperature (RT) dynamic characteristics of the SAQD laser for several initial carrier relaxation lifetimes which corresponds to phonon bottleneck at different inhomogeneous broadening-FWHMs (a) 10 meV and (b) 20 meV.

As shown in fig (5), with increase of carrier relaxation lifetime, relaxation oscillation peak and uncompleted steady-state photons decrease and turn-on delay increases. This is because, the injected carriers are consumed in the WL and thus do not contribute to lasing oscillation. For the larger inhomogeneous broadening, turn-on delay increases, uncompleted steady-state photons and the relaxation oscillation peak decrease, because the number of QD groups gets larger, as a result, carriers that emit into the central mode decrease.

CONCLUSION

Considering the homogeneous and inhomogeneous broadenings of the linear optical gain, we solved the rate equations numerically using fourth-order Runge-Kutta method and analyzed the dynamic and static-characteristics of InGaAs/GaAs SAQD-LD. Dynamic-characteristics and uncompleted steady-state photons improve as the current increases. Threshold current and turn-on delay elevate and relaxation oscillation frequency decreases as the homogeneous broadening increases. Uncompleted steady-states appear at homogeneous broadenings comparable or equal to inhomogeneous broadening. We showed that there is a special homogeneous broadening for a special injected current that the QD laser has maximum of output power. Besides, for larger initial relaxation lifetimes (phonon bottleneck) and inhomogeneous broadenings, turn-on delay increases and uncompleted steady-state photons decline.

ACKNOWLEDGEMENT

With special thank full from Azad University Aliabad Katoul Branch that this article is resulting from research project entitled "Simulation of dynamic and static characteristics of semiconductor nano-structure quantum dot lasers"published in this university.

REFERENCES

1. Steiner, T. 2004. Semiconductor nano structures for optoelectronic applications, Artech House.
2. Bimberg, D., 1999. Quantum Dot Heterostructures', John Wiley and Sons Inc.
3. Sugawara, M., 1998. Part of the SPIE Conference on Physics and Simulation of optoelectronic devises VI', 3283: 88.
4. Sugawara, M., 2005. Appl. Phys., 97: 043523.
5. Sugawara, M., 1999. Self -Assembled InGaAs/GaAs Quantum Dots', Academic Press, p: 60.
6. Sugawara, M., 2000. Phys. Rev. B, 61: 7595.
7. Sugawara, M., 1997. Applied. Phys. Lett., 71: 2791.
8. Tan, C.L., 2008. Comput. Mater. Sci., (2008) doi: 10.1016/*j. commatsci.* 01: 049.
9. Tan, C.L. and Y. Wang, 2007. Applied Phys. Lett., 91: 061117.